JACS
JOURNAL OF THE AMERICAN CHEMICAL SOCIETY
Article
pubs.acs.org/JACS

Solution ^{31}P NMR Study of the Acid-Catalyzed Formation of a Highly Charged $\{U_{24}Pp_{12}\}$ Nanocluster, $[(UO_2)_{24}(O_2)_{24}(P_2O_7)_{12}]^{48-}$, and Its Structural Characterization in the Solid State Using Single-Crystal Neutron Diffraction

Mateusz Dembowski,[†] Travis A. Olds,[‡] Kristi L. Pellegrini,[‡] Christina Hoffmann,[§] Xiaoping Wang,[§] Sarah Hickam,[‡] Junhong He,[∥] Allen G. Oliver,[†] and Peter C. Burns*[,†,‡]

[†]Department of Chemistry and Biochemistry, University of Notre Dame, Notre Dame, Indiana 46556, United States
[‡]Department of Civil and Environmental Engineering and Earth Sciences, University of Notre Dame, Notre Dame, Indiana 46556, United States
[§]Chemical and Engineering Materials Division, Oak Ridge National Laboratory, Oak Ridge, Tennessee 37831, United States
[∥]Instrument and Source Division, Oak Ridge National Laboratory, Oak Ridge, Tennessee 37831, United States

Supporting Information

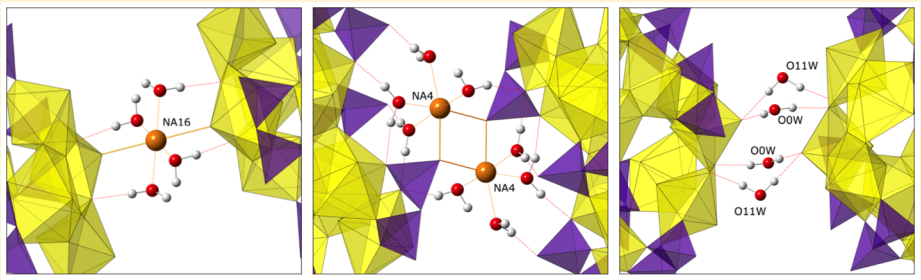

ABSTRACT: The first neutron diffraction study of a single crystal containing uranyl peroxide nanoclusters is reported for pyrophosphate-functionalized $Na_{44}K_6[(UO_2)_{24}(O_2)_{24}(P_2O_7)_{12}][IO_3]_2{\cdot}140H_2O$ (**1**). Relative to earlier X-ray studies, neutron diffraction provides superior information concerning the positions of H atoms and lighter counterions. Hydrogen positions have been assigned and reveal an extensive network of H-bonds; notably, most O atoms present in the anionic cluster accept H-bonds from surrounding H_2O molecules, and none of the surface-bound O atoms are protonated. The D_{4h} symmetry of the cage is consistent with the presence of six encapsulated K cations, which appear to stabilize the lower symmetry variant of this cluster. ^{31}P NMR measurements demonstrate retention of this symmetry in solution, while *in situ* ^{31}P NMR studies suggest an acid-catalyzed mechanism for the assembly of **1** across a wide range of pH values.

INTRODUCTION

Since their discovery in 2005, the family of uranyl peroxide cage clusters has expanded to more than 60 varieties.[1−3] These clusters, which self-assemble in water under ambient conditions and contain as many as 124 uranyl moieties, have potential applications in the nanoscale control of uranium in the nuclear fuel cycle.[4] The curvature of these clusters is attributed to the pliability of the $\mu{:}\eta^2{-}\eta^2$ peroxide bridge present between uranyl ions ($U{-}O_2{-}U$), which was recently highlighted in a study of 15 peroxide-bridged uranyl dimers with $U{-}O_2{-}U$ dihedral angles ranging from 134° to 180°.[5] A subclass of these clusters containing pyrophosphate (Pp) bridges presents a rare opportunity to study them using ^{31}P NMR. A recent study of the $\{U_{24}Pp_{12}\}$ anion provided insights into its solution dynamics, showcasing its remarkable solution stability at elevated temperatures.[6] Moreover, formation of Pp-functionalized clusters represents a unique chemical system describing interactions of polyuranates with oligophosphates. This is noteworthy because the synthesis of Pp-bearing transition metal polyoxometalates (POMs) is synthetically challenging due to the acid and metal catalyzed hydrolysis of Pp.[7−11]

To date, single-crystal X-ray diffraction (XRD) has been the primary means of elucidating the structures of uranyl peroxide cage clusters. Difference-Fourier maps obtained from these experiments are dominated by scattering from U, and consequently the structure models lack information about the location of H, Li, and often Na atoms. While the charge-balancing role of these species is indisputable, their importance in cluster assembly, and their impact on cluster physical and chemical properties are still poorly understood. Here we begin to address some of these issues by turning to single-crystal neutron diffraction for crystals of a Na/K salt of $\{U_{24}Pp_{12}\}$ and solution ^{31}P NMR. The neutron scattering factors for the

Received: April 19, 2016
Published: June 20, 2016

DOI: 10.1021/jacs.6b04028
J. Am. Chem. Soc. 2016, 138, 8547−8553

various constituents present in **1** are more favorable for a more complete structural elucidation while ^{31}P NMR provides insight into the solution behavior of uranyl peroxide pyrophosphate species under cluster forming conditions. It is noteworthy that the structure of $\{U_{24}Pp_{12}\}$ is the largest metal-oxide cluster and the first actinyl-oxide cluster studied using single-crystal neutron diffraction.[12−15] The limited number of neutron-determined cluster structures in the literature may be attributed to the difficulty of obtaining large, high quality crystals.[16]

EXPERIMENTAL SECTION

Caution! *Depleted uranium was used during the course of these experiments. ^{238}U is an α emitter, and all experiments were carried out in a laboratory designated for the use of radioactive isotopes. Exposure of ^{238}U to thermal neutrons can lead to formation of ^{239}Pu via neutron capture reaction followed by two beta decays.*

General Considerations. Commercially obtained uranyl nitrate hexahydrate (UN, $UO_2(NO_3)_2{\cdot}6H_2O$) was purified by heating at 450 °C to obtain UO_3, which was subsequently dissolved in 14 M HNO_3. The resulting solution was evaporated to dryness on a hot plate and, subsequently, the solid was recrystallized from ultrapure water. All other reagents were used as received from commercial suppliers. Clusters are abbreviated as $\{U_nPp_m\}$, where n corresponds to the number of $[UO_2(O_2)]$ units and m is the number of $P_2O_7^{4-}$ bridges. The presence of K in the final product originated from N-$(CH_2CH_3)_4OH$ (TEAOH) contamination, as shown by via ICP-OES (see Supporting Information, Table S2). The choice of TEAOH as the source of OH^- in the synthesis of $U_{24}Pp_{12}$ was driven by its bulky and non-templating nature.[5,17] Among a variety of different acids considered in this study, only HIO_3 yielded crystals of suitable size and quality for neutron diffraction study.

$Na_{44}K_6[(UO_2)_{24}(O_2)_{24}(P_2O_7)_{12}][IO_3]_2{\cdot}140H_2O$ (1). Combining 5.0 mL of 0.5 M $UO_2(NO_3)_2$ (International Bio-Analytical Industries) with 5.0 mL 30% H_2O_2 (EMD Millipore) resulted in the precipitation of studtite $(UO_2O_2(H_2O)_2{\cdot}2H_2O)$. Addition of 6.25 mL 2.0 M $Na_4P_2O_7$ (Spectrum) followed by titration using 40% TEAOH (Sigma-Aldrich) yielded a clear orange solution with pH = 11.00. Acidification of this mixture using 0.5 M HIO_3 (Alfa Aesar) resulted in a solution with pH = 7.10. Evaporation of the solution yielded diffraction quality crystals after 2 weeks. Yield: 0.26g (18.6% based on U). Elemental analyses (%) by ICP-OES, found (calculated): Na 7.2 (7.5), K 1.7 (1.7), U 41.5 (42.5), P 5.5 (5.5)

Single-Crystal X-ray Diffraction. XRD data were collected at 100 K using a Bruker APEX single-crystal diffractometer with monochromated Mo Kα X-ray radiation. Data collection, corrections, and solution were performed in accordance with previously published procedures.[5]

Single-Crystal Neutron Diffraction. Neutron diffraction data were collected using the TOPAZ single-crystal time-of-flight (TOF) Laue diffractometer at the Spallation Neutron Source (SNS), Oak Ridge National Laboratory.[18] A block-shaped hydrogenated crystal of **1**, with dimensions of 1.5 × 1.25 × 0.75 mm^3, was mounted on the tip of a polyimide capillary using fluorinated grease, and transferred to the TOPAZ goniometer for data collection at 100 K. To ensure good coverage and redundancy, data were collected using 17 crystal orientations optimized with *CrystalPlan* software[19] for an estimated 98% coverage of symmetry-equivalent reflections of the triclinic cell. Each crystal orientation was measured for approximately 8 h. The integrated raw Bragg intensities were obtained using the 3-D ellipsoidal Q-space integration in accordance with previously reported methods.[20] Data reduction including neutron TOF spectrum, Lorentz, and detector efficiency corrections was carried out with the *ANVRED3* program.[21] A spherical absorption correction was applied with μ = 1.150 + 1.022 λ cm^{-1}. The reduced data were saved as SHELX HKLF2 format in which the wavelength is recorded separately for each reflection. Data were not merged. The initial neutron structure was refined using the X-ray structure as a starting point: specifically the positions of the constituents of the $\{U_{24}Pp_{12}\}$ cage and some interstitial species. The positions of O and H atoms of water molecules were located from difference-Fourier maps calculated from the neutron data. The neutron crystal structure was refined using a mixture of anisotropic and isotropic treatments to convergence using the *SHELXL-14/7* program[22,23] in *WinGx*.[24] Some of the water molecules exhibited partial occupancy and/or were refined with O−H distance constraints (some of the oxygen atoms, and the associated H atoms were assigned half occupancy with O−H distances restrained to 0.96(1) Å). Neutron crystallographic data for **1**: triclinic, $P\bar{1}$, a = 21.886(4) Å, b = 22.379(4) Å, c = 22.717(4) Å, α = 62.227(2)°, β = 87.715(2)°, γ = 61.278(2)°, V = 8387(2) Å^3, Z = 2, T = 100(2) K; total number of measured reflections 94 809, number of unique reflections 31 629, independent/observed reflections after being merged by SHELXL according to the crystal symmetry 14 914/14 900; R_1(obs) = 0.1061 for reflections with $I > 2\sigma(I)$ and wR_2(all) = 0.2626 for all reflections. The goodness of fit on F^2 was 1.100.

NMR Measurements. Spectra were recorded using a 500 MHz Varian INOVA spectrometer (11.74 T) with a power level attenuation of 56 dB, a pulse length of 14.8 ms, 124 scans, and a relaxation time (d1) of 5 s. Standard spectra of **1** were obtained by dissolving 20 mg of crystalline material in 1 mL of 99.8% D_2O. Formation of $\{U_{24}Pp_{12}\}$ was probed over a wide range of pH values by titration of initially alkaline stock solution (pH = 11, described above) using 0.5 M HIO_3 until the target pH was achieved. Initial NMR measurements were taken 1 h subsequent to pH adjustment, by which time any off-gassing had subsided. ^{31}P chemical shifts are reported relative to neat H_3PO_4 placed in an NMR insert tube at 298 K. Solutions obtained from variable pH self-assembly studies were done with a D_2O insert that allowed for signal locking and shimming.

Characterization Data. Raman and IR spectra of **1** with peak assignments are available in Figures S1 and S2, and Table S1. TGA results are available in Figure S3. ESI-MS spectra, as well as peak deconvolution and assignments, are in Figure S4 and Table S3, respectively. Crystallographic data are available in Tables S4−S8, and in CIF format.

RESULTS AND DISCUSSION

The reaction of aqueous $UO_2(NO_3)_2$, H_2O_2 and $Na_4P_2O_7$ with TEAOH followed by acidification using HIO_3 results in self-assembly of uranyl polyhedra into pyrophosphate-functionalized uranyl peroxide clusters across a wide range of pH values. X-ray and neutron diffraction showed that the crystalline product of this reaction is the mixed Na and K salt of $\{U_{24}Pp_{12}\}$: $Na_{44}K_6[(UO_2)_{24}(O_2)_{24}(P_2O_7)_{12}][IO_3]_2{\cdot}140H_2O$ (**1**).

The coordination environment of each uranyl (UO_2^{2+}) unit in **1** is hexagonal bipyramidal, with the apexes of the polyhedron defined by two *-yl* oxygens, and equatorial vertices by two μ:η^2-η^2 peroxide [O_2^{2-}] and one bridging bis-bidentate pyrophosphate [$P_2O_7^{4-}$, Pp] (Figure 1c,d). The structure of the $\{U_{24}Pp_{12}\}$ anion consists of 24 uranyl monoperoxide $[UO_2(O_2)]$ subunits arranged into six internally linked (via μ:η^2-η^2 O_2^{2-}) tetramers $[(UO_2)_4(O_2)_4]$ $\{U_4\}$. Cross-linkage of $\{U_4\}$ units by 12 bis-bidentate pyrophosphate [$P_2O_7^{4-}$] bridges results in a hollow, oblong (e = 0.63)[6] cluster with D_{4h} molecular symmetry (Figure 1a,b) and 1.44 × 1.8 × 1.85 nm^3 molecular dimensions as defined by the distance between the centers of two outer *-yl* oxygens. The symmetry reflects the presence of two distinct types of $\{U_4\}$ units, convex (four units) and concave (two units), relative to the center of mass of the cluster. Convex units are characterized by two ∼140° (Figure 2a) and two ∼100° (Figure 2b) U−Pp−U dihedral angles, whereas concave units contain four U−Pp−U dihedral angles of ∼100°. Here we define the U−Pp−U dihedral angle as the angle between two planes, one of which passes through a U atom and both P atoms of the corresponding Pp unit, and the

DOI: 10.1021/jacs.6b04028
J. Am. Chem. Soc. 2016, 138, 8547−8553

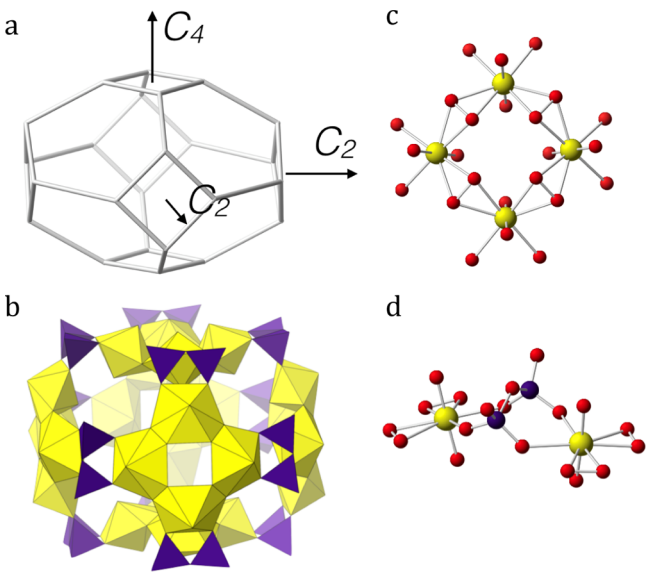

Figure 1. Graphical (a) and polyhedral (b) representations of the cluster in the mixed Na and K salt of $\{U_{24}Pp_{12}\}$. Ball-and-stick representation of the $\{U_4\}$ unit (c) and bis-bidentate pyrophosphate bridges. U, P, and O atoms are shown as yellow, purple, and red spheres, respectively. In (a), lines represent linkages between polyhedra.

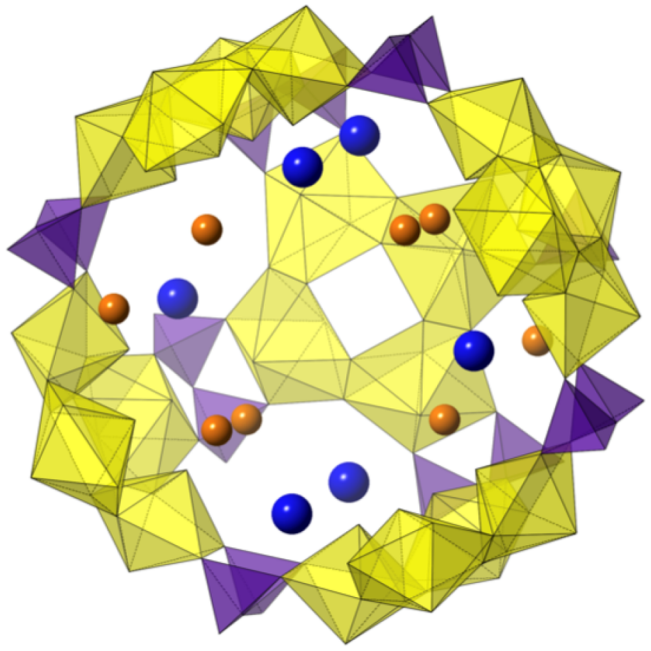

Figure 3. Polyhedral/ball-and-stick representation of the distribution of cations in the central cavity of $\{U_{24}Pp_{12}\}$. U and Pp polyhedra are shown in yellow and purple, respectively. Na and K atoms are shown as orange and blue spheres, respectively. Water molecules are omitted for clarity.

other plane that passes through the other U atom that is shared with the Pp unit and both P atoms.

The central cavity of the K/Na salt of $\{U_{24}Pp_{12}\}$ contains 14 cations (six K, eight Na) and approximately 29 positionally disordered water molecules (Figure 3). All internal cations are located near the cluster surface and have variable coordination environments defined by a combination of *-yl*, U−**O**$_2$−U, and U−**O**−P oxygens and water molecules. Similar to Keplerates, uranyl peroxide cages contain molecular pores that potentially allow for exchange of internal cations with the surrounding environment.[25] Specifically, $\{U_{24}Pp_{12}\}$ contains eight quasi-hexagonal pores $\{U_6P_3O_9\}$ that are occupied by six K and two Na cations (Figure 4a,b). The inter-cluster space is populated by the remaining Na cations (36 indicated by chemical analysis, 31 of which were crystallographically located) and two symmetry-related IO_3^- located on the periphery of the concave $\{U_4\}$ units (Figure 5). The IO_3^- units show typical trigonal pyramidal geometry and are involved in two I−O_{yl} electrostatic interactions at 2.928 and 3.016 Å. Bond-valence sums obtained from the neutron structure are summarized in Table 1.[26−28]

The ^{31}P NMR spectrum of **1** yields two signals at 3.45 and 4.28 ppm, integrated to give a 2:1 ratio, respectively (Figure 6a), consistent with the crystallographically determined structure showing two distinct types of U−Pp−U dihedral angles (Figure 6c). Results obtained from the *in situ* self-assembly study are summarized in Figure 6b. Briefly, signals corresponding to K/Na $\{U_{24}Pp_{12}\}$ are present in all spectra (3.45 and 4.28 ppm) except at pH = 11 and pH = 5. The presence of additional signals in the ^{31}P NMR spectra likely indicates co-existence of other pyrophosphate functionalized uranyl peroxide clusters or simpler pyrophosphate bearing species.

An earlier study of the $\{U_{24}Pp_{12}\}$ anion proposed composition $[(UO_2)_{24}(O_2)_{24}(HP_2O_7)_6(H_2P_2O_7)_6]^{30-}$, indicating that some of the terminal pyrophosphate oxygen atoms are protonated. The single-crystal XRD used in these earlier experiments did not provide any information about the H atom positions, and the assignment was based on chemical analyses.[6,29] The neutron data presented herein provide specific information on H atom and Na atom positions. Before discussing these in detail, we first consider the overall distribution of bond strengths within the cage structure. The collinear *-yl* oxygens are strongly bonded to U^{6+} with their bond providing ∼1.6 valence units (*vu*) to satisfy the 2 *vu* requirement of O^{2-} in the bond-valence formalism.[26] Given that a typical O−H bond is ∼0.8 *vu*, the *-yl* oxygens are unlikely

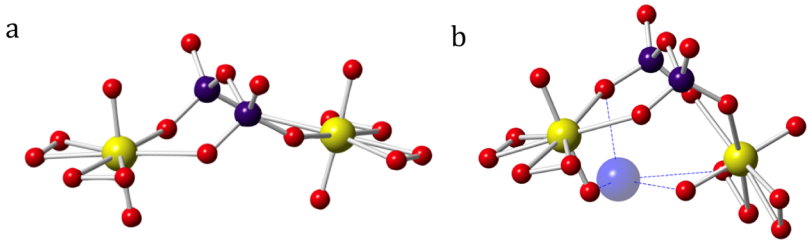

Figure 2. Ball-and-stick representation of two unique types of pyrophosphate bridges present in the structure of **1**. U, P, O, and K atoms are represented by yellow, purple, red, and blue spheres, respectively.

DOI: 10.1021/jacs.6b04028
J. Am. Chem. Soc. 2016, 138, 8547−8553

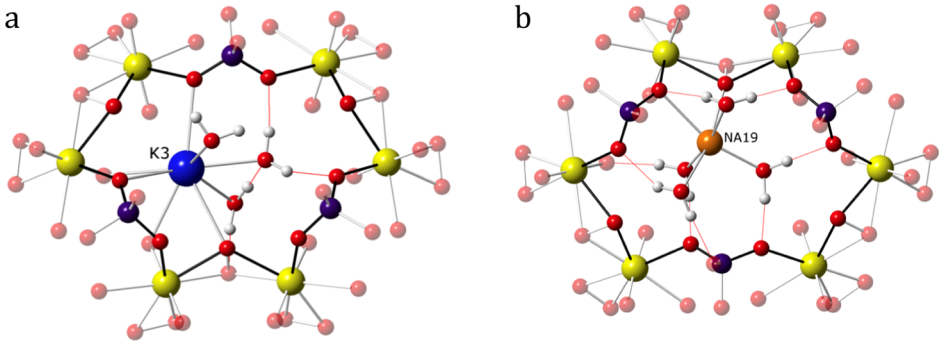

Figure 4. Ball-and-stick representation of some of the quasi-hexagonal $\{U_6P_3O_9\}$ pores present in **1**. U, P, O, K, Na, and H atoms are shown as yellow, purple, red, blue, orange, and white spheres, respectively. H-bonds are shown in red.

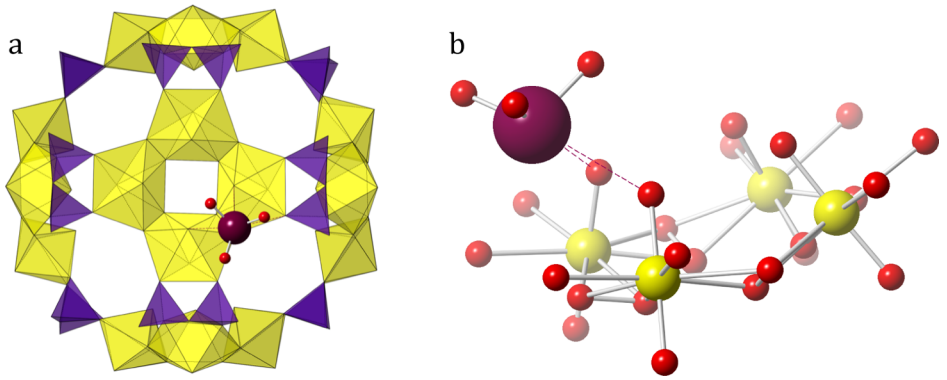

Figure 5. (a) Polyhedral/ball-and-stick representation of the IO^{3-} group located near the concave $\{U_4\}$ subunit. (b) Ball-and-stick representation of the interactions between an IO^{3-} molecule and two *-yl* oxygen atoms present in the $\{U_4\}$ subunit. U and Pp polyhedra are shown in yellow and purple, respectively. U, O, and I atoms are shown as yellow, red, and burgundy, respectively.

Table 1. Summary of Bond-Valence Sums Obtained from the Neutron Diffraction Study of 1

element	bond valence	std dev	R_{ij}	b	ref
U	6.3176	0.0561	2.042	0.506	20
P	4.9543	0.0779	1.617	0.370	21
I	4.9749	N/A	0.440	1.990	22
-yl **O**	1.8515	0.1256	2.042	0.506	20
U−**O**−P	2.0107	0.0693	2.042	0.506	21
P−**O**−P	2.0395	0.0672	1.617	0.370	21
P═O	2.0392	0.0784	1.617	0.370	21
O−**O**	1.2623	0.1153	2.042	0.506	20

to be protonated, and such protonation has never been demonstrated in uranyl chemistry. However, the *-yl* oxygens can act as acceptors of H-bonds, and are often bound to highly coordinated alkali cations. In the case of terminal oxygen atoms of the pyrophosphate units, the P−O bonds are ∼1.3 *vu*, hence it is possible for them to be protonated. In a situation where they are not protonated, their bond-valence deficiency can be satisfied by accepting H-bond(s), and/or by bonding to alkali metal cations. The remaining O atoms present in the cage structure are either peroxide O atoms, each of which are bonded to two U^{6+} cations, or pyrophosphate O atoms that are either bonded to two P^{5+} cations (P−O−P) or one P^{5+} and one U^{6+} cations (U−O−P). In these cases, their bond-valence requirements are largely met.

We now examine the detailed positions of selected H atoms in the neutron structure starting with atom O76. The environment about O76 is a distorted tetrahedron defined by one P and three Na atoms (Figure 7) with a computed bond-valence sum of 1.94 *vu*. The second terminal oxygen present in the same pyrophosphate unit (O70, Figure 7), in the absence of any H atoms, would have a bond-valence sum of 1.35 *vu*. The neutron diffraction data show O70 to be an H-bond acceptor that is surrounded by three partially occupied water molecules. The calculated bond-valence sum of O70, including H-bond contributions, is 1.97 *vu*. Likewise, the other terminal pyrophosphate O atoms present in **1** interact with Na atoms and the H atoms of water molecules, resulting in similar environments. The exception is O89, for which the coordination sphere contains one Na atom and two partially occupied water molecules. Note that none of the terminal O atoms of the cluster are protonated. Other O atoms present in the pyrophosphate bridges (U−**O**−P and P−**O**−P) accept H-bonds from as many as two water molecules, resulting in an average bond-valence sum of 2.04 *vu*.

Determination of the positions of the H atoms in the structure of **1** has revealed a multitude of previously unobserved cluster-water interactions. Specifically, the majority of O atoms present in peroxide bridges accept H-bonds from one water molecule, with an average H-acceptor distance of 1.84 Å and an average H−O−O angle of 109.8°. Of 24 crystallographically unique peroxide oxygen atoms, only one is bonded to Na, whereas three neither accept H-bonds nor bond to Na atoms. Among the 24 crystallographically unique *-yl* oxygens, only two show no interactions beyond those with U^{6+}, 15 are bonded to Na, six are bonded to K, and nine are H-bond acceptors. Some *-yl* oxygen atoms are bonded to cations and simultaneously accept H-bonds (e.g., O46), resulting in an average bond-valence sum of 1.85 *vu*.

DOI: 10.1021/jacs.6b04028
J. Am. Chem. Soc. 2016, 138, 8547−8553

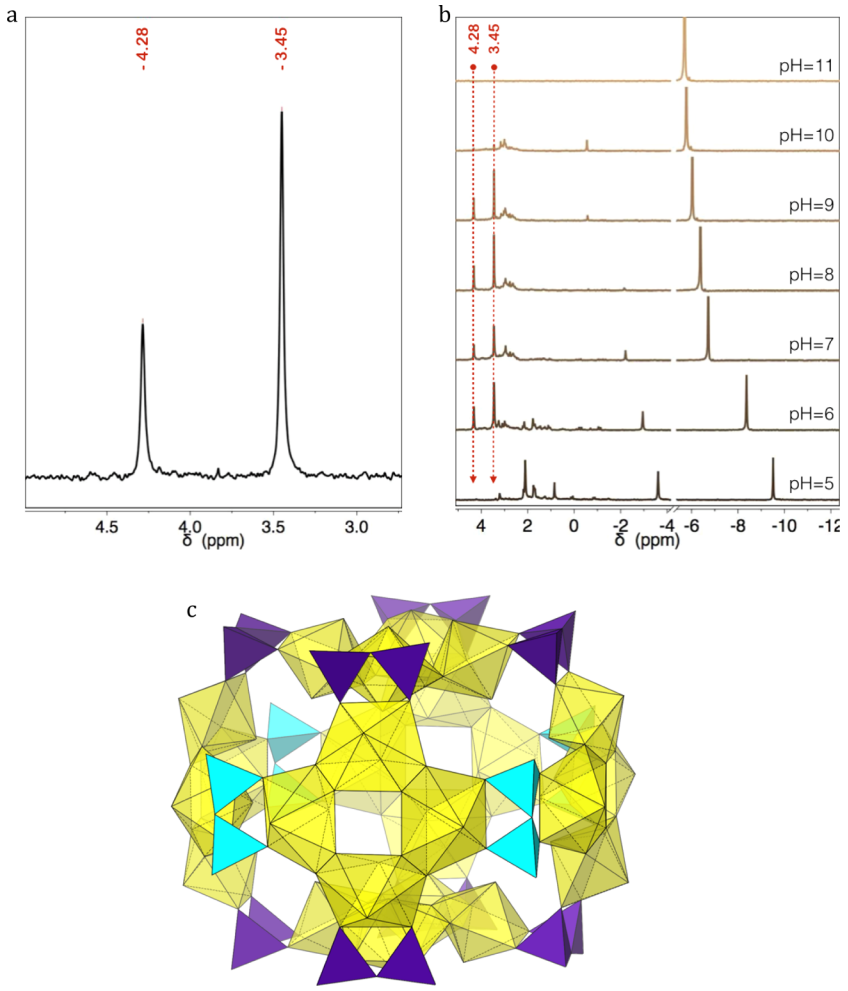

Figure 6. (a) ^{31}P NMR spectrum of pure Na/K {U24Pp12}. (b) Stacked ^{31}P NMR spectra obtained from in situ study of {U24Pp12} assembly as a function of pH. (c) Two inequivalent ^{31}P sites of Na/K {U24Pp12} marked as teal (4 Pp groups, 4.28 ppm signal) and purple (8 Pp groups, 3.45 ppm signal). U polyhedra are shown in yellow.

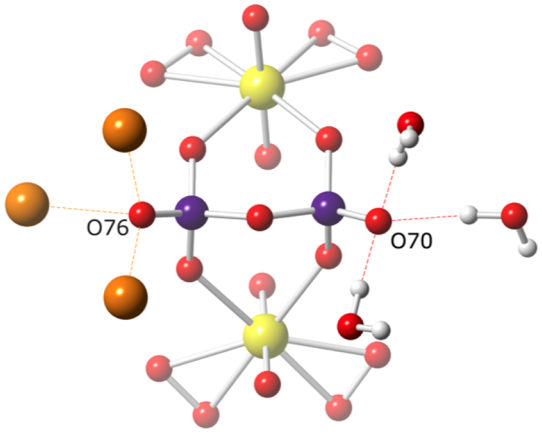

Figure 7. Ball-and-stick representation of terminal O atoms present in a typical Pp unit of **1** and its surroundings. U, P, O, Na, and H are shown as yellow, purple, red, orange, and white spheres, respectively.

In addition to their charge-balancing role, Na cations present in the interstitial space facilitate linkages between cluster molecules present in the crystal. For example, Na16 links two {$U_{24}Pp_{12}$} clusters by directly bonding to *-yl* oxygen atoms (O−Na−O, 180°), one from each cluster, with a U−O−Na angle of 144.85°, and an O−O distance of 5.039 Å (Figure 8, left). A second direct Na bridge (Na4) is observed between pyrophosphate units (Figure 8, center), with an average O−Na−O angle of 87.32°, and an O−O distance of 3.306 Å. The bridging of two clusters additionally occurs through two symmetry-related water molecules (O0W, O11W) that link an *-yl* oxygen of one cluster with a peroxide bridge of another by H-bonding (Figure 8, right), resulting in a cluster-to-cluster (nearest O−O) distance of 3.343 Å.

The correlation between the geometry of the structural features present in **1** and signals observed in solution ^{31}P NMR specta indicate its remarkable solution stability and show that the anion retains its D_{4h} symmetry upon dissolution. In the solid state, the existence of the second, less obtuse U−Pp−U dihedral angle (~100°, Figure 2b) is likely caused by numerous cation−anion type interactions occurring between internally located K cations and the surface *-yl*, U−$\mathbf{O_2}$−U, and U−**O**−P oxygen atoms present in discrete {U_4} units (Figure 9). Among topologically related clusters (e.g., U_{60}−$U_{60}Ox_{30}$, U_{50}−$U_{50}Ox_{20}$, where Ox = oxalate),[30,31] only $U_{24}Pp_{12}$ and $U_{24}PCP_{12}$ (PCP = methylenediphosphonate) assume lower molecular symmetry than their non-functionalized counterparts.[1] We hypothesize that the unusual conformation observed in the structure of **1** is a direct result of the pliability of Pp bridges combined with the presence of K cations in the system. In their absence, the {$U_{24}Pp_{12}$} anion would likely assume a higher symmetry

DOI: 10.1021/jacs.6b04028
J. Am. Chem. Soc. 2016, 138, 8547−8553

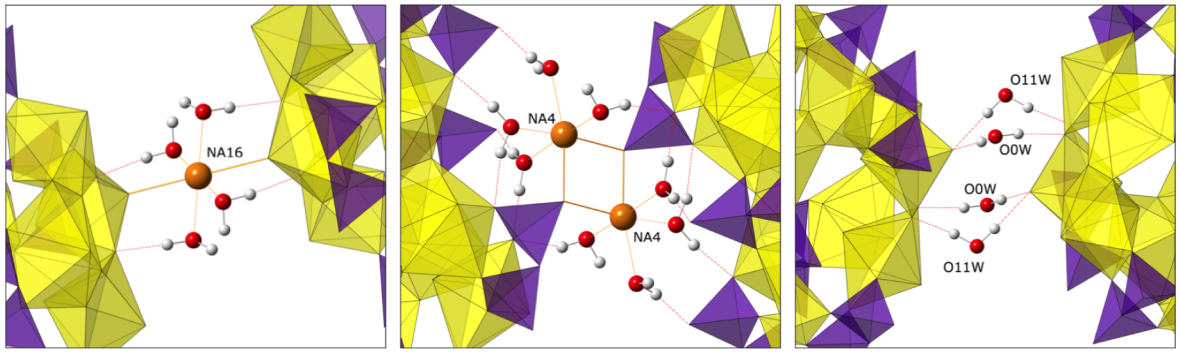

Figure 8. Polyhedral/ball-and-stick representations of some of the direct cluster-to-cluster bridging motifs found in **1**. Uranium and pyrophosphate polyhedra are shown in yellow and purple, respectively. Na, O, and H atoms are shown as orange, red, and white spheres, respectively.

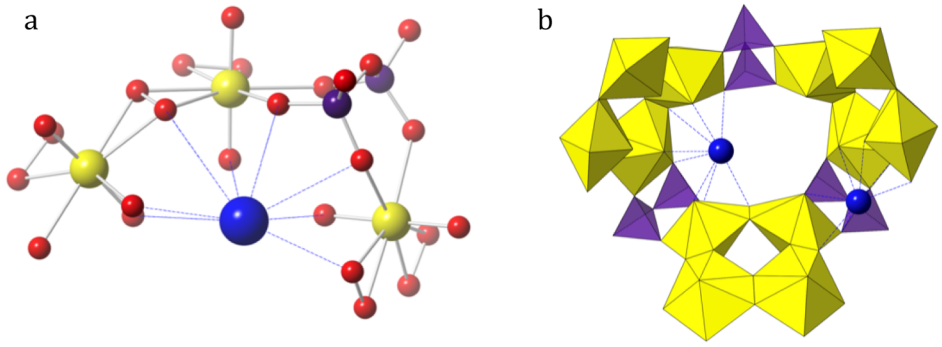

Figure 9. Polyhedral/ball-and-stick representations of interactions between K cations and multiple O atoms found in discrete {U4} units. Uranium and pyrophosphate polyhedra are shown in yellow and purple, respectively. U, P, O, and K atoms are shown as yellow, purple, red, and blue spheres, respectively.

conformation (O_h), similar to that observed in the solid-state structure of the $\{U_{24}\}$ anion.[32]

^{31}P NMR results obtained in the present study indicate formation of the $\{U_{24}Pp_{12}\}$ anion across pH values ranging from pH = 10 to pH = 6 (Figure 6b). Moreover, formation of **1** is only observed in acidified reaction mixtures, hinting at the acid-catalyzed nature of this reaction, while the lack of a signal corresponding to the $\{U_{24}Pp_{12}\}$ anion at pH = 5 suggest its limited stability under acidic conditions. Although the identity of additional signals observed in the ^{31}P NMR spectra has not been determined, it is likely they represent other types of pyrophosphate-functionalized clusters present in solution (e.g., $U_{32}Pp_{16}$) or simpler pyrophosphate/phosphate bearing species. The apparent polydispersity of solution, as determined by ^{31}P NMR, agrees with previous SAXS studies conducted on $\{U_xPp_y\}$ reaction mixtures.[29]

CONCLUSIONS

Neutron diffraction data have allowed for the unequivocal assignment of the $\{U_{24}Pp_{12}\}$ protonation state and localization of almost all cations. The positions of cations located within the structure, along with trends seen in functionalized uranyl peroxide systems, allow us to conclude that the conformation of the $\{U_{24}Pp_{12}\}$ anion (D_{4h} symmetry) is a direct result of strong K−O interactions within its cavity. *In situ* ^{31}P NMR studies have shown $\{U_{24}Pp_{12}\}$ to assemble across a wide range of pH values with a limited stability under acidic conditions.

ASSOCIATED CONTENT

Supporting Information

The Supporting Information is available free of charge on the ACS Publications website at DOI: 10.1021/jacs.6b04028.

Crystallographic information file for **1** (CIF)
Raman and infrared spectra, chemical characterization (ICP-OES), thermogravimetric analysis, electrospray ionization mass sprectra, and additional crystallographic information (PDF)

AUTHOR INFORMATION

Corresponding Author

*pburns@nd.edu

Notes

The authors declare no competing financial interest.

ACKNOWLEDGMENTS

This material is based upon work supported as a part of the Materials Science of Actinides Center, an Energy Frontier Research Center funded by the U.S. Department of Energy, Office of Science, Office of Basic Energy Sciences, under Award No. DE-SC0001089. NMR measurements were conducted at the Magnetic Resonance Research Center at the University of Notre Dame. Electrospray ionization mass spectra were collected at the Mass Spectrometry and Proteomics Facility at University of Notre Dame. Raman spectroscopy and thermogravimetric analysis measurements were collected at the Materials Characterization Facility of the Center for Sustainable Energy at the University of Notre Dame. Work performed at the ORNL Spallation Neutron Source's TOPAZ

DOI: 10.1021/jacs.6b04028
J. Am. Chem. Soc. 2016, 138, 8547−8553

single-crystal diffractometer was supported by the Scientific User Facilities Division, Office of Basic Energy Sciences, U.S. Department of Energy, under Contract No. DE-AC05-00OR22725 with UT-Battelle, LLC.

REFERENCES

(1) Qiu, J.; Burns, P. C. *Chem. Rev.* **2013**, *113*, 1097.
(2) Ling, J.; Hobbs, F.; Prendergast, S.; Adelani, P. O.; Babo, J.-M.; Qiu, J.; Weng, Z.; Burns, P. C. *Inorg. Chem.* **2014**, *53*, 12877.
(3) Qiu, J.; Ling, J.; Jouffret, L.; Thomas, R.; Szymanowski, J. E. S.; Burns, P. C. *Chem. Sci.* **2014**, *5*, 303.
(4) Wylie, E. M.; Peruski, K. M.; Weidman, J. L.; Phillip, W. A.; Burns, P. C. *ACS Appl. Mater. Interfaces* **2014**, *6*, 473.
(5) Qiu, J.; Vlaisavljevich, B.; Jouffret, L.; Nguyen, K.; Szymanowski, J. E. S.; Gagliardi, L.; Burns, P. C. *Inorg. Chem.* **2015**, *54*, 4445.
(6) Johnson, R. L.; Ohlin, C. A.; Pellegrini, K.; Burns, P. C.; Casey, W. H. *Angew. Chem., Int. Ed.* **2013**, *52*, 7464.
(7) Kortz, U.; Jameson, G. B.; Pope, M. T. *J. Am. Chem. Soc.* **1994**, *116*, 2659.
(8) Kortz, U.; Pope, M. T. *Inorg. Chem.* **1994**, *33*, 5643.
(9) Lavrov, A. V.; Pobedina, A. B.; Rozanov, I. A. *Zh. Neorg. Khim.* **1980**, *25*, 1047.
(10) Li, Q.; Zhang, S. W. *Z. Anorg. Allg. Chem.* **2005**, *631*, 2490.
(11) du Peloux, C.; Mialane, P.; Dolbecq, A.; Marrot, J.; Secheresse, F. *Angew. Chem., Int. Ed.* **2002**, *41*, 2808.
(12) Teller, R. G.; Wilson, R. D.; McMullan, R. K.; Koetzle, T. F.; Bau, R. *J. Am. Chem. Soc.* **1978**, *100*, 3071.
(13) Hart, D. W.; Teller, R. G.; Wei, C. Y.; Bau, R.; Longoni, G.; Campanella, S.; Chini, P.; Koetzle, T. F. *J. Am. Chem. Soc.* **1981**, *103*, 1458.
(14) Dolbecq, A.; du Peloux, C.; Auberty, A. L.; Mason, S. A.; Barboux, P.; Marrot, J.; Cadot, E.; Secheresse, F. *Chem. - Eur. J.* **2002**, *8*, 349.
(15) Evans, H. T.; Prince, E. *J. Am. Chem. Soc.* **1983**, *105*, 4838.
(16) Blakeley, M. P.; Langan, P.; Niimura, N.; Podjarny, A. *Curr. Opin. Struct. Biol.* **2008**, *18*, 593.
(17) Vlaisavljevich, B.; Gagliardi, L.; Burns, P. C. *J. Am. Chem. Soc.* **2010**, *132*, 14503.
(18) Jogl, G.; Wang, X.; Mason, S. A.; Kovalevsky, A.; Mustyakimov, M.; Fisher, Z.; Hoffman, C.; Kratky, C.; Langan, P. *Acta Crystallogr., Sect. D: Biol. Crystallogr.* **2011**, *67*, 584.
(19) Zikovsky, J.; Peterson, P. F.; Wang, X. P.; Frost, M.; Hoffmann, C. *J. Appl. Crystallogr.* **2011**, *44*, 418.
(20) Schultz, A. J.; Jorgensen, M. R. V.; Wang, X.; Mikkelson, R. L.; Mikkelson, D. J.; Lynch, V. E.; Peterson, P. F.; Green, M. L.; Hoffmann, C. M. *J. Appl. Crystallogr.* **2014**, *47*, 915.
(21) Schultz, A. J.; Srinivasan, K.; Teller, R. G.; Williams, J. M.; Lukehart, C. M. *J. Am. Chem. Soc.* **1984**, *106*, 999.
(22) Sheldrick, G. M. *Acta Crystallogr., Sect. A: Found. Crystallogr.* **2008**, *64*, 112.
(23) Gruene, T.; Hahn, H. W.; Luebben, A. V.; Meilleur, F.; Sheldrick, G. M. *J. Appl. Crystallogr.* **2014**, *47*, 462.
(24) Farrugia, L. J. *J. Appl. Crystallogr.* **2012**, *45*, 849.
(25) Mueller, A.; Gouzerh, P. *Chem. - Eur. J.* **2014**, *20*, 4862.
(26) Burns, P. C.; Ewing, R. C.; Hawthorne, F. C. *Can. Mineral.* **1997**, *35*, 1551.
(27) Brown, I. D.; Altermatt, D. *Acta Crystallogr., Sect. B: Struct. Sci.* **1985**, *41*, 244.
(28) Sidey, V. *Acta Crystallogr., Sect. B: Struct. Sci.* **2009**, *65*, 99.
(29) Ling, J.; Qiu, J.; Sigmon, G. E.; Ward, M.; Szymanowski, J. E. S.; Burns, P. C. *J. Am. Chem. Soc.* **2010**, *132*, 13395.
(30) Ling, J.; Wallace, C. M.; Szymanowski, J. E. S.; Burns, P. C. *Angew. Chem., Int. Ed.* **2010**, *49*, 7271.
(31) Ling, J.; Qiu, J.; Burns, P. C. *Inorg. Chem.* **2012**, *51*, 2403.
(32) Burns, P. C.; Kubatko, K. A.; Sigmon, G.; Fryer, B. J.; Gagnon, J. E.; Antonio, M. R.; Soderholm, L. *Angew. Chem., Int. Ed.* **2005**, *44*, 2135.

DOI: 10.1021/jacs.6b04028
J. Am. Chem. Soc. 2016, 138, 8547−8553